A High Purity Fused Silica (HPFS) Glass Substrate based 77 GHz 4 × 4 Butler Matrix for Automotive Radars

Ronak Sakhiya, Sazzadur Chowdhury
Department of Electrical and Computer Engineering
University of Windsor
Windsor, Ontario, Canada
e-mail: sakhiya@uwindsor.ca

***Abstract*— This paper presents the design of a 77 GHz 4 × 4 Butler matrix on a High Purity Fused Silica (HPFS) glass substrate for automotive radar applications. The design and 3D Finite Element Method (FEM) simulation of the 4 × 4 Butler matrix beamformer has been conducted using an industry-standard CAD tool Advanced Design System (ADS) from Keysight™ Technologies. The 4 × 4 Butler matrix having a footprint area of 9.5 mm × 8.3 mm with 0.8-micrometer copper cladding thickness has been designed using a 0.2 mm thick HPFS glass as the microstrip dielectric substrate. The simulated insertion loss is –8 ± 2 dB. The return loss and isolation of the input ports are both below –20 dB respectively. This 4 × 4 Butler matrix can generate beam patterns at an elevation angle of –42°, –15°, 0°, 15°, and 42° when a corresponding port is excited. The maximum and minimum main lobe gain achieved are 20.322 dB and 16.763 dB respectively. These characteristics make the designed Butler matrix suitable for automotive radar applications, such as Adaptive Cruise Control (ACC), Collision Mitigation (CM), blind-spot detection, vehicle tracking, and pre-crash warning system.**

Keywords- Butler matrix; microstrip beamformer; antenna array; beam steering; 3D FEM simulations.

I. INTRODUCTION

The automotive radars have become the key enabling technology for Adaptive Cruise Control (ACC), autonomous driving, and Collision Mitigation (CM) applications for vehicles. Early automotive radars were designed to operate at 24 GHz center frequency. However, the narrow bandwidth of such radars was not suitable to achieve necessary range and velocity accuracies. Their large size made the system bulkier as well. Consequently, the automotive manufacturers focused on developing automotive radars operating at 76 GHz – 81 GHz frequency range to improve the range and velocity accuracies at a lower cost and smaller form factor following the regulations and recommendations of European Telecommunications Standard Institute (ETSI) and Federal Communications Commission (FCC) [1], [2]. Additionally, as the millimeter waves at high frequencies undergo very less absorption in human tissues due to their lower penetration through the human skin [3], the 76 GHz – 81 GHz is safer compared to 24 GHz.

In any communication system, it is necessary to adjust the antenna beams in appropriate directions so that the electromagnetic signals are transmitted and received between the end users with minimum signal loss. Modern communication systems consist of multibeam array antennas which are typically backed by Radio Frequency (RF) beamformers to achieve the target of beam steering with wide angle coverage [4]. There are several RF beamformers, such as Butler matrix [5], Rotman lens [6], [7], Blass matrix [8] and Nolen matrix [9], [10]. Out of all these, the advantages of Butler matrix forces to be an ideal candidate in terms of size, manufacturing costs, bandwidth, reliability, and reciprocity; therefore, it is widely used in several applications such as Internet of Things (IoT), Wi-Fi, base station, satellite communications as well as automotive radars [11]–[19].

The authors in [4] presented an excellent comprehensive analysis of available Butler matrices to conclude that a bilayer Butler matrix designed using meta-material substrate-based transmission lines is more suitable for 5G applications. However, the design and fabrication of transmission lines with meta-material substrates for each component of the Butler matrix is complex and demand further technological advances.

In [19], the design and fabrication of a 77 GHz planar Butler matrix implemented using a Substrate Integrated Waveguide (SIW) technology has been presented. However, the fabrication of the device is complex as the implementation requires several metal vias to direct the propagation of electromagnetic signals to realize the beamforming and beam steering capability.

Investigation by the authors of this paper show that as the microstrip transmission lines are comparatively easier to design and fabricate, the design and fabrication complexity of SIW based Butler matrix can be minimized by realizing an appropriate geometry microstrip Butler matrix with necessary input and output ports to achieve desired spatial resolutions. Due to easier small form factor fabrication of such microstrip Butler matrices, they can be easily integrated to realize small form factor simpler but superior functionality automotive radars.

Microstrip technology involves use of an appropriate substrate sandwiched between a conducting layer and a ground layer. The authors in [20], [21] recommended that glass substrates are better suited for W-band applications due to their superior performance compared to organic and ceramic substrates in terms of reliability, surface roughness,

 ISBN: 978-1-68558-006-3

loss tangent, thickness, dimensional and thermal stability. Accordingly, a HPFS glass substrate from Corning™ has been selected as the substrate material to design the target 77 GHz center frequency 4 × 4 microstrip Butler matrix. The selected substrate has a low loss tangent (tan δ) of 0.0005, surface roughness < 10 Å, and a dielectric constant (ε_r) of 3.82 at 77 GHz [22], [23].

In this context, this paper presents the design and simulation results of a HPFS glass substrate-based 77 GHz 4 × 4 microstrip Butler matrix. The rest of the paper has been organized in the following manner: Section 1 describes the state-of-the-art of available Butler matrices and its need to be used in automotive radars. In Section 2, the theory and working principle of Butler matrix is described followed by the design and results of microstrip components and complete 4 × 4 Butler matrix. The beamforming capability of the designed 4 × 4 Butler matrix is also displayed. Section 3 and 4 describes the conclusion and acknowledgement followed by references section.

II. MICROSTRIP BUTLER MATRIX DESIGN

The Butler matrix is a passive beamforming network having *N* input ports (beam ports) and *N* output ports, where $N = 2^n$ and *n* is a positive non-zero integer. Each input port is connected to all output ports with high isolation between input ports. During operation, an RF signal is fed at one of the input ports. The corresponding signals received at the output ports are fed to an antenna array such that the phase difference among the antenna array elements remains the same. The block diagram of a 4 × 4 Butler matrix composed of 90˚ hybrid couplers, crossovers, and 45˚ phase shifters is shown in Figure 1.

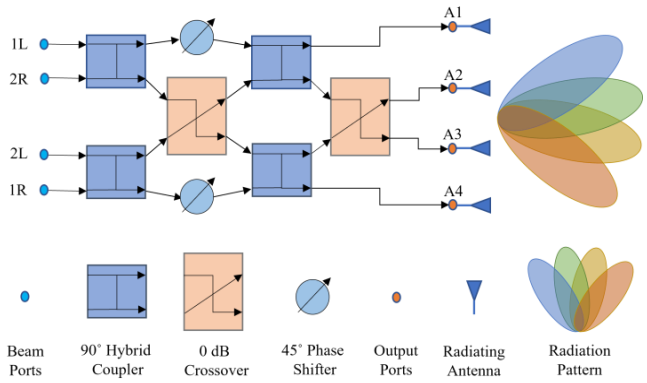

Figure 1. Beamforming by 4 × 4 Butler matrix.

In Figure 1, the Butler matrix is feeding a four-element linear antenna array. The detailed theories of operation a Butler matrix are available in [4], [5], [11]–[18].

The operational phase parameters of the 4 × 4 Butler matrix in Figure 1 are provided in Table I. The radiation patterns are observed at a constant azimuthal angle (φ) = 90˚. The equations to determine values of phase difference (Δϕ) and beam angle (θ) are available in [18].

The design challenge is to determine the optimized dimensions of the HPFS glass substrate-based 77 GHz microstrip transmissions lines to realize the 90˚ hybrid couplers, crossovers, and 45˚ phase shifters.

TABLE I PHASE DISTRIBUTION IN 4 × 4 BUTLER MATRIX

	Beam Ports			
Output ports	**1L**	**2R**	**2L**	**1R**
A1	–45	–135	–90	–180
A2	–90	0/360	–225/135	–135
A3	–135	–225/135	0/360	–90
A4	–180	–90	–135	–45
Phase difference (Δϕ)	45	–135	135	–45
Beam angle (θ)	–14.47	48.6	–48.6	14.47

*All values are in degrees.

It was found through simulation studies by the authors that the microstrip width at the port terminals must be between 0.1 mm and 0.2 mm to excite the 77 GHz RF signals into the Butler matrix network with minimum return loss. The characteristic impedance of microstrip lines in the Butler matrix needs to be within 70 Ω and 100 Ω.

A. 90˚ Hybrid Coupler

The 90˚ hybrid coupler is a four-port directional coupler which is used to divide the input power equally at respective output ports and provide 90˚ phase difference across the output ports. Figure 2 shows the layout of the designed 90˚ hybrid coupler at 77 GHz in ADS. The corresponding widths and lengths are found by repetitive parametric optimization techniques in ADS and are listed in Table II.

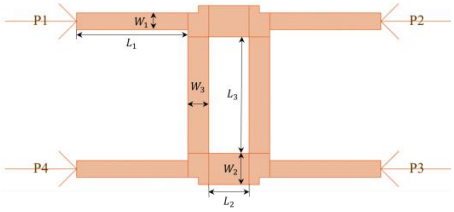

Figure 2. Layout of the designed microstrip 90˚ hybrid coupler.

TABLE II DIMENSIONS OF DESIGNED MICROSTRIP 90 HYBRID COUPLER

Parameter	W_1	L_1	W_2	L_2	W_3	L_3
Values(mm)	0.118	0.779	0.145	0.816	0.22	0.28

*All values are in mm.

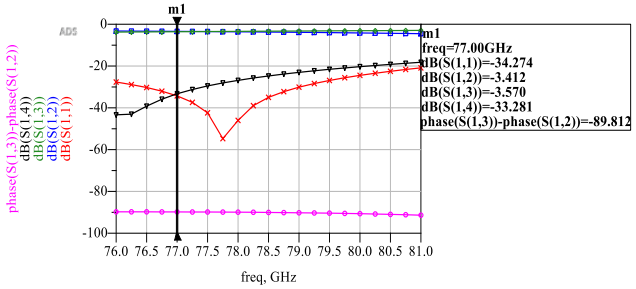

Figure 3. Performance of the designed 90˚ hybrid coupler.

The 3D FEM simulation results of the 90˚ hybrid coupler at 77 GHz frequency are shown in Figure 3. The phase shift between the output signals at port 2 and 3 of the 90˚ hybrid coupler is 89.812 degrees. The simulated insertion loss between port 1 and port 2 is –3.412 dB and that between port 1 and port 3 is –3.57 dB. The return loss is –34.274 dB and isolation of port 1 and port 4 or port 2 and port 3 is –33.281 dB.

B. Crossover

A crossover is also a directional coupler used to spatially switch a signal in a planar geometry without any coupling. The typical design of a microstrip crossover involves the cascading two 90° hybrid couplers. However, as per the design requirements of 4 × 4 Butler matrix, the design of 0 dB crossover was modified by connection of 90˚ curved bends at each port and optimized in ADS using 3D FEM simulations to get ideally 0 dB crossover. Figure 4 shows the layout of the designed microstrip crossover.

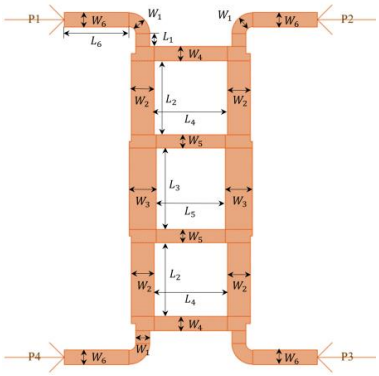

Figure 4. Layout of the designed crossover.

The corresponding values of widths and lengths of crossover are provided in Table III. These values are found by repetitive iterations of parametric optimization techniques in ADS.

TABLE III DIMENSIONS OF DESIGNED CROSSOVER.

Parameters	W_1	W_2	W_3	W_4	W_5	W_6
Values(mm)	0.116	0.192	0.226	0.12	0.11	0.122

Parameters	L_1	L_2	L_3	L_4	L_5	L_6
Values(mm)	0.107	0.618	0.686	0.616	0.582	0.547

*All values are in mm.

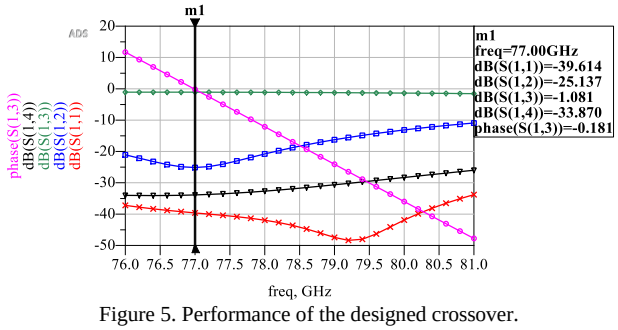

Figure 5. Performance of the designed crossover.

The performance values of the designed crossover shown in Figure 5 are optimum at frequency of 77 GHz. The isolation of port 1 and port 4 is –33.87 dB and that for port 1 and port 2 is –25.137 dB. The corresponding return loss is –39.614 dB. The insertion loss and phase shift between port 1 and port 3 is –1.081 dB and –0.181˚.

C. 45˚ Phase Shifter

The implemented phase shifter is a microstrip transmission line that is used to adjust the phases of the output signals of the various components in the Butler matrix. To obtain the phase distribution as listed in Table I, it is necessary to design 45˚ phase shifters.

The 45˚ phase shifter as shown in Figure 6 was designed by optimizing the distance between the ports P1 and P2 and then tuning the length L_2. The corresponding values of width and lengths are given in Table IV.

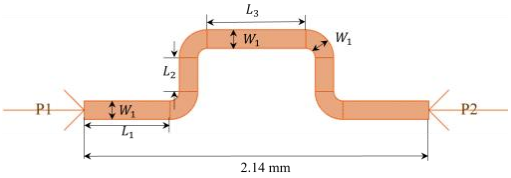

Figure 6. Layout of the designed 45˚ phase shifter.

TABLE IV. DIMENSIONS OF DESIGNED 45˚ PHASE SHIFTER.

Parameter	W_1	L_1	L_2	L_3
Values(mm)	0.118	0.532	0.136	0.616

*All values are in mm.

The performance of the designed 45˚ phase shifter is shown in Figure 7. The insertion loss and phase difference between the input port and output port at 77 GHz frequency are –0.156 dB and –45˚ respectively.

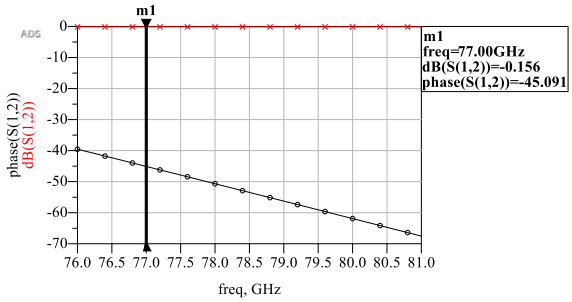

Figure 7. Performance of the designed 45˚ phase shifter.

D. 4 × 4 Butler Matrix S-parameter Simulation

After successfully optimizing the designs of 90° hybrid coupler, crossover, and 45° phase shifter, the components were then integrated as per the block diagram shown in Figure 1 to realize the complete 4 × 4 Butler matrix as shown in Figure 8. The beam ports 1L, 2R, 2L, and 1R are the same as P1, P2, P3, and P4 respectively. The total footprint area of the completed 4 × 4 Butler matrix is 9.5 mm × 8.3 mm. Figure 9 shows the S-parameters of the

 ISBN: 978-1-68558-006-3

designed Butler matrix in ADS obtained through 3D FEM simulations.

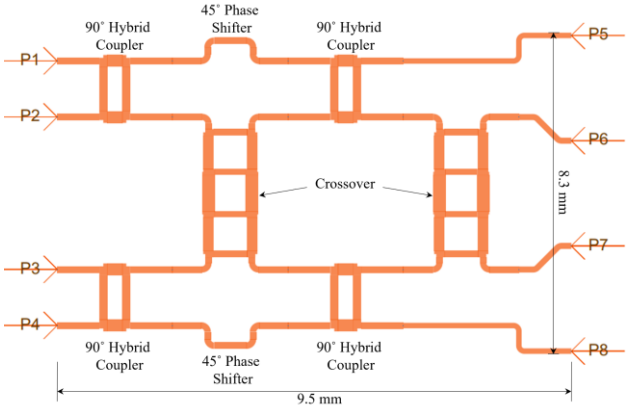

Figure 8. Layout of the complete 4 × 4 Butler matrix.

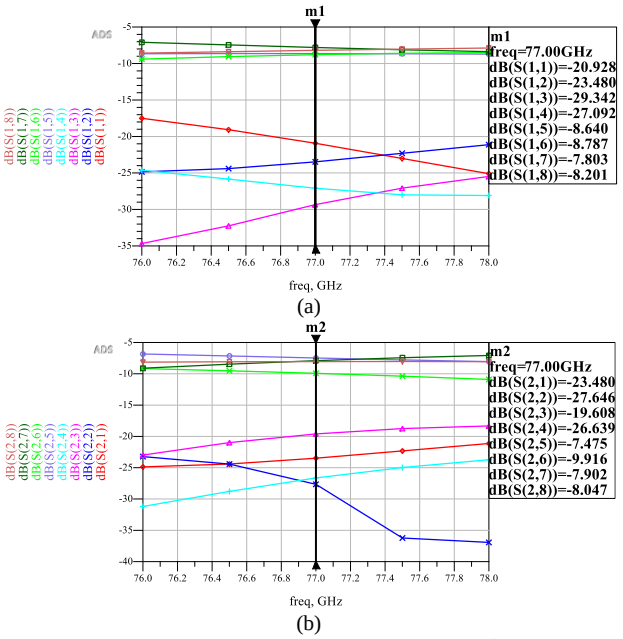

Figure 9. (a) Isolation, return loss, and insertion losses of the designed 4 × 4 Butler matrix obtained through 3D FEM simulations in ADS with Port 1 or Port 4 excited. (b) Isolation, return loss, and insertion losses of the designed 4 × 4 Butler matrix the obtained through 3D FEM simulations in ADS with Port 2 or Port 3 excited.

The insertion loss between port 1 or 4 and ports 5, 6, 7, and 8 are between –7.5 dB and –8.8 dB. The insertion loss between port 2 or 3 and ports 5, 6, 7, and 8 are between –7.4 dB and –10 dB. The return losses at respective ports are below –20 dB and isolation of adjacent input ports is below –20 dB.

E. 4 × 4 Butler Matrix Beampatterns

A microstrip antenna array is designed to validate the beamforming capability of the designed 4 × 4 Butler matrix. Figure 10 shows the 4 × 4 Butler matrix layout with inset-fed microstrip antenna array of four elements. The antenna design dimensions are provided in Table V. The dimensions of microstrip inset fed antenna are also found by repetitive iterations of parametric optimization in ADS.

TABLE V DIMENSIONS OF MICROSTRIP INSET FED ANTENNA

Parameter	d_{feed}	d	L_{feed}	L_a
Values(mm)	1.945	1.126	0.843	0.945

Parameter	S	W_a	W_f	W_{in}
Values(mm)	0.187	0.819	0.163	0.118

*All values are in mm.

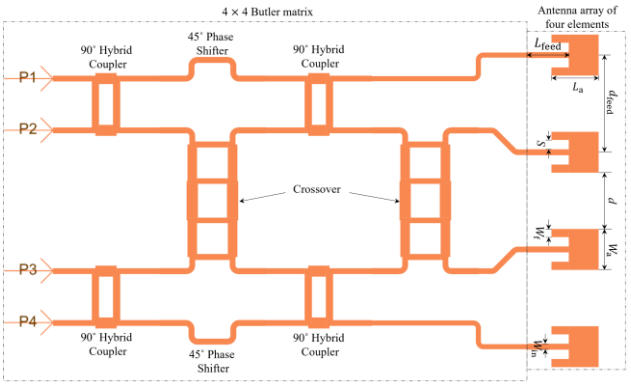

Figure 10. Layout of the complete 4 × 4 Butler matrix with antenna array

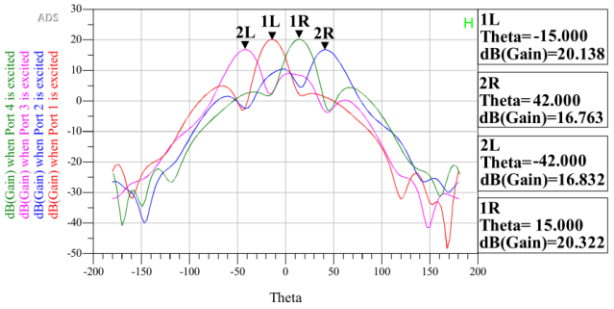

Figure 11. Rectangular plot of beamforming by the designed 4 × 4 Butler matrix.

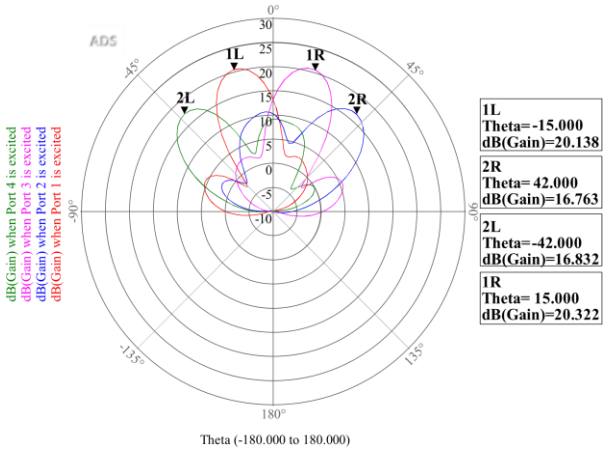

Figure 12. Polar plot of beamforming by the designed 4 × 4 Butler matrix.

When input ports 1, 2, 3 and 4 are excited individually, the beam patterns are observed at θ = –15˚, 42˚, –42˚ and

15˚, respectively for azimuth angle (φ) = 90˚ as shown in Figure 11 and Figure 12. The beam angle phase error is ±7˚ from the expected beam angle phase given in Table 1. The maximum gain of 20.322 dB is observed on excitation of port 4. The minimum gain of 16.763 dB is observed on excitation of port 2. The difference between main lobe level and side lobe levels is higher than 14 dB when port 1 (or 1L) and port 4 (or 1R) is excited but lower than 10 dB when port 2 (or 2R) and port 3 (or 2L) are excited.

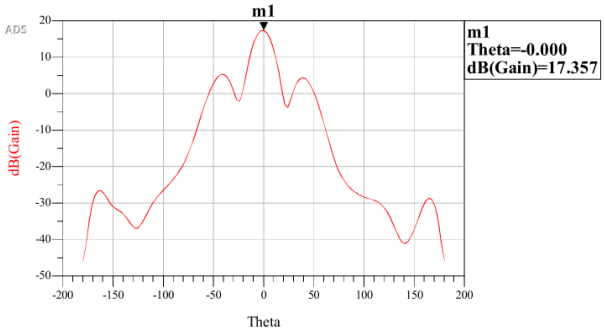

Figure 13. Rectangular plot of a beam pattern when all input ports of the designed 4 × 4 Butler matrix are excited.

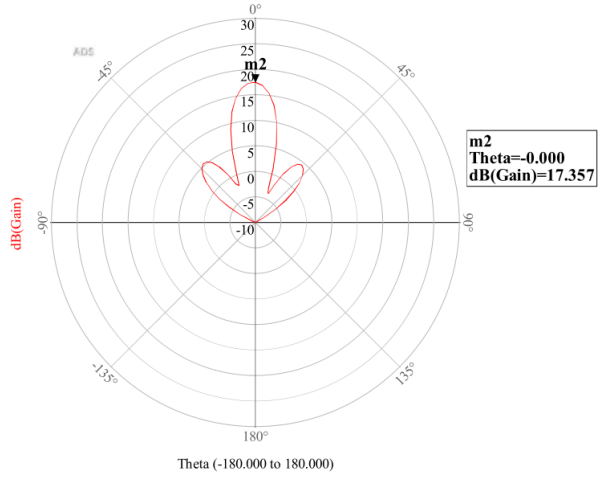

Figure 14. Polar plot of a beam pattern when all input ports of the designed 4 × 4 Butler matrix are excited.

When all the input ports are excited, the signal is received at output ports with $\Delta\phi = 0^{\circ}$ and hence, the beam pattern is observed at $\theta = 0^{\circ}$ as shown in Figure 13 and Figure 14. The respective gain of the main lobe is 17.357 dB. The difference between main lobe level and side lobe levels is significantly more than 11 dB.

III. Conclusion

The designed 77 GHz microstrip 4 × 4 Butler matrix on a 0.2 mm thick HPFS glass substrate has the potential to provide superior performance at a lower cost, smaller size, and thickness to realize compact radars to improve road safety and driving comfort for vehicles with advanced driver-assistance system (ADAS) and autonomous vehicles. It was observed that the glass substrate from Corning™ has superior loss characteristics to minimize insertion loss at high frequencies. However, optimization of the phase characteristics and insertion losses in a 3D FEM simulation environment requires more than 500 GB of memory. The time taken by ADS solvers to run one simulation is computationally extensive. Further optimization is necessary to improve the insertion loss and the phase error. Initial investigation shows that the device can be fabricated using a standard microfabrication technique, such as the lift-off process available in any standard microfabrication facility. The device will be fabricated and tested once the optimization process is completed.

Acknowledgement

This research work was supported by the Natural Science and Engineering Research Council of Canada (NSERC)'s discovery grant number RGPIN 293218. The authors also acknowledge the collaborative research support provided by the IntelliSense Corporation, Lynnfield, MA, Angstrom Engineering, ON, and the CMC Microsystems, Canada.

References

[1] J. Hasch, et al, "Millimeter-Wave Technology for Automotive Radar Sensors in the 77 GHz Frequency Band," in IEEE Trans. Microw. Theory and Techn., vol. 60, no. 3, pp. 845-860, March 2012, doi: 10.1109/TMTT.2011.2178427.

[2] S. Chatterjee, "A 77 GHz BCB Based High Performance Antenna Array for Autonomous Vehicle Radars," Electronic Theses and Dissertations. 7505, Dept. Elect. Comp. Eng., Univ. Windsor, Ontario, Canada.2018. [Online]. Available: https://scholar.uwindsor.ca/etd/7505. Retrieved: June, 2022.

[3] T. Wu, T. S. Rappaport, and C. M. Collins, "The human body and millimeter wave wireless communication systems: Interactions and implications," 2015 IEEE International Conference on Communications (ICC), London, UK, 2015, pp. 2423-2429, doi: 10.1109/ICC.2015.7248688.

[4] A. K. Vallappil, M. K. A. Rahim, B. A. Khawaja, N. A. Murad, and M. G. Mustapha, "Butler Matrix Based Beamforming Networks for Phased Array Antenna Systems: A Comprehensive Review and Future Directions for 5G Applications," in IEEE Access, vol. 9, pp. 3970-3987, 2021, doi: 10.1109/ACCESS.2020.3047696.

[5] J. Butler and R. Lowe. "Beam-forming matrix simplifies design of electronically scanned antennas." Electronic Design no.9, 1961, pp. 170-173.

[6] W. Rotman and R. Turner, "Wide-angle microwave lens for line source applications," in IEEE Trans. on Antennas and Propag., vol. 11, no. 6, pp. 623-632, November 1963, doi: 10.1109/TAP.1963.1138114.

[7] A. Attaran and S. Chowdhury, "Fabrication of a 77GHz Rotman Lens on a High Resistivity Silicon Wafer Using Lift-Off Process," in Int. J. Antennas and Propag., Vol 2014, Article ID 471935, pp. 1-9.

[8] J. Blass, "Multidirectional antenna - A new approach to stacked beams," in proc. of 1958 IRE Int. Conv. Rec., New York, NY, USA. 1960. pp. 48-50, doi: 10.1109/IRECON.1960.1150892.

[9] J. Nolen, "Synthesis of multiple beam networks for arbitrary illuminations," Ph.D. dissertation, Radio Division, Bendix Corp., Baltimore, MD, USA, Apr. 1965.

 ISBN: 978-1-68558-006-3

[10] H. Ren, H. Zhang, Y. Jin, Y. Gu, and B. Arigong, "A Novel 2-D 3×3 Nolen Matrix for 2-D Beamforming Applications," in IEEE Trans. on Microw. Theory and Techn., vol. 67, no. 11, pp. 4622-4631, Nov. 2019, doi: 10.1109/TMTT.2019.2917211.

[11] H. Nord, "Implementation of an 8x8-Butler Matrix in Microstrip", Diploma Thesis, Technische Universitat Wien, Vienna, Austria, 1998.

[12] R. D. Cerna and M. A. Yarlequé, "Design and implementation of a wideband 8×8 Butler Matrix for AWS and PCS 1900 MHz beamforming networks," in proc. of 2015 IEEE International Wireless Symposium (IWS 2015), Shenzhen, 2015, pp. 1-4, doi: 10.1109/IEEE-IWS.2015.7164630

[13] A. Shastrakar and U. Sutar, "Design and Simulation of Microstrip Butler Matrix Elements Operating at 2.4GHz for Wireless Applications", in Int. J. Scientific & Eng. Res., Volume 7, Issue 5, May-2016, pp. 1528-1531, ISSN 2229-5518.

[14] M. SalarRahimi and G. Vandenbosch, "Beam steerable subarray with small footprint for use as building block in wall-mounted indoor wireless infrastructure," IET Microw., Antennas & Propag., vol. 13, no. 4, pp. 526–531, Mar. 2019.

[15] T. Djerafi, N. Fonseca, and K. Wu, "Design and implementation of a planar 4×4 butler matrix in SIW technology for wideband applications," in proc. of The 40th European Microw. Conf., Paris, 2010, pp. 910-913, doi: 10.23919/EUMC.2010.5616642.

[16] H. Habibi, "Design of a 4x4 Butler Matrix for Vehicle Radar Beamforming Antenna systems at 24 GHz." Master's Thesis, Telecomunn. Eng. University of Gaza, Palestine, 2014.

[17] S. Orakwue, R. Ngah, T. Rahman, and H. Al-Khafaji, "A 4 × 4 Butler Matrix for 28 GHz Switched Multi-Beam Antenna," in Int. J. Eng. and Technol. (IJET), ISSN: 0975-4024, Vol 7 No 2, Apr-May 2015.

[18] I. Idrus, T. Latef, N. Aridas, and M. Talep, "Design and characterization of a compact single-layer multibeam array antenna using an 8×8 Butler matrix for 5G base station applications." in Turkish J. Electr. Eng. Comput. Sci. 28 (2020): pp. 1121-1134.2020.

[19] T. Djerafi and K. Wu, "A Low-Cost Wideband 77-GHz Planar Butler Matrix in SIW Technology," in IEEE Trans. on Antennas and Propag., vol. 60, no. 10, pp. 4949-4954, Oct. 2012, doi: 10.1109/TAP.2012.2207309.

[20] M. Rehman, S. Ravichandran, S. Erdogan, and M. Swaminathan, "W-band and D-band Transmission Lines on Glass Based Substrates for Sub-THz Modules," in proc. of 2020 IEEE 70th Electron. Compon. Techn. Conf. (ECTC), Orlando, FL, USA, 2020, pp. 660-665, doi: 10.1109/ECTC32862.2020.00109.

[21] Corning HPFS® Fused Silica. Datasheet, Corning Inc., May 2017. [Online] Available: https://www.corning.com/media/worldwide/csm/documents/CorningHPFSFusedSilicaWafer_PI.pdf. Retrieved: June, 2022

[22] Y. Uemichi, et al, "A ultra low-loss silica-based transformer between microstrip line and post-wall waveguide for millimeter-wave antenna-in-package applications," in proc. of 2014 IEEE MTT-S Int. Microw. Symp. (IMS2014), Tampa, FL, USA, 2014, pp. 1-3, doi: 10.1109/MWSYM.2014.6848279.

[23] Y. Uemichi, et al, "Characterization of 60-GHz silica-based post-wall waveguide and low-loss substrate dielectric," in proc. of 2016 Asia-Pacific Microw. Conf. (APMC), New Delhi, India, 2016, pp. 1-4, doi: 10.1109/APMC.2016.7931433.

 ISBN: 978-1-68558-006-3